Journal of Neuroscience Methods 407 (2024) 110127

Contents lists available at ScienceDirect

Journal of Neuroscience Methods

journal homepage: www.elsevier.com/locate/jneumeth

Short communication

Phase-amplitude coupling detection and analysis of human 2-dimensional neural cultures in multi-well microelectrode array in vitro

Yousef Salimpour [a], William S. Anderson [a], Raha Dastgheyb [b], Shiyu Liu [b], Guo-li Ming [c], Hongjun Song [c], Nicholas J. Maragakis [b,1], Christa W. Habela [b,*,1]

[a] Functional Neurosurgery Laboratory, Department of Neurosurgery, Johns Hopkins School of Medicine, Baltimore, Maryland, USA
[b] Department of Neurology, Johns Hopkins School of Medicine, Baltimore MD, USA
[c] 1Department of Neuroscience and Mahoney Institute for Neurosciences, Perelman School of Medicine, Philadelphia, PA, USA

ARTICLE INFO

Keywords:
Cross-frequency coupling
Phase-amplitude coupling
Multielectrode array
induced pluripotent stem cells (iPSC)
human neuronal culture
epilepsy
Parkinson's disease
human astrocyte

ABSTRACT

Background: Human induced pluripotent stem cell (hiPSC)- derived neurons offer the possibility of studying human-specific neuronal behaviors in physiologic and pathologic states *in vitro*. It is unclear whether cultured neurons can achieve the fundamental network behaviors required to process information in the brain. Investigating neuronal oscillations and their interactions, as occurs in cross-frequency coupling (CFC), addresses this question.

New methods: We examined whether networks of two-dimensional (2D) cultured hiPSC-derived cortical neurons grown with hiPSC-derived astrocytes on microelectrode array plates recapitulate the CFC that is present *in vivo*. We employed the modulation index method for detecting phase-amplitude coupling (PAC) and used offline spike sorting to analyze the contribution of single neuron spiking to network behavior.

Results: We found that PAC is present, the degree of PAC is specific to network structure, and it is modulated by external stimulation with bicuculline administration. Modulation of PAC is not driven by single neurons, but by network-level interactions.

Comparison with existing methods: PAC has been demonstrated in multiple regions of the human cortex as well as in organoids. This is the first report of analysis demonstrating the presence of coupling in 2D cultures.

Conclusion: CFC in the form of PAC analysis explores communication and integration between groups of neurons and dynamical changes across networks. *In vitro* PAC analysis has the potential to elucidate the underlying mechanisms as well as capture the effects of chemical, electrical, or ultrasound stimulation; providing insight into modulation of neural networks to treat nervous system disorders *in vivo*.

1. Introduction

Our understanding of human neurologic development and disease is confounded by the fact that the study of human neurons *in vivo* is limited by patient safety factors. Invasive intracranial recordings used in the diagnosis and management of neurologic disorders, such as epilepsy, allow significant observations to be made about human neural network behaviors. However, there are limited opportunities to test hypotheses about the mechanisms and clinical implications of this neural activity, specifically when it comes to single-cell activity that may underlie network changes. Computational models have been the mainstay of hypothesis testing, but without understanding the underlying behavior and biology of single cells that generate this activity, these models are imperfect (Cash and Hochberg, 8 2015).

In human neurologic disorders, such as epilepsy and Parkinson's disease (PD), cross-frequency coupling (CFC), which describes the interactions of neural oscillations at different frequencies with one another, is one parameter to describe network behavior. The presence or absence of CFC has been implicated as an important feature of functional neural network activity based on an association with both normal processing behaviors and pathologic states, such as seizures (Salimpour and Anderson, 2019). CFC is present and increased at the onset of seizures, but not during or in between seizures.It is also present and increased during complex cognitive processing (Canolty and Knight, 2010).

* Correspondence to: 600 N. Wolfe Street, Meyer 2-147, Baltimore, MD 21231, USA.
E-mail address: chabela1@jh.edu (C.W. Habela).
[1] Co-Senior Authors

https://doi.org/10.1016/j.jneumeth.2024.110127
Received 3 October 2023; Received in revised form 13 March 2024; Accepted 25 March 2024
Available online 13 April 2024

Phase-amplitude coupling (PAC), a form of cross frequency coupling, describes the relationship between the phase of low frequency oscillations and the amplitude of high frequency activity. In the motor cortex of PD patients, excessive abnormal PAC between the phase of beta rhythms and the amplitude of high frequency gamma activity has been demonstrated and strong correlations between PAC and motor symptom severity have been observed (de Hemptinne et al., 2013). Further, modulation of motor symptoms with levodopa or deep brain stimulation has been associated with a reduction in this PAC (Salimpour et al., 2022). This suggests that not only is PAC a biomarker for disease states, but that modulation of PAC may modulate symptoms. However, the underlying cellular processes contributing to this coupling in normal and pathologic states are not fully understood.

Human induced pluripotent stem cell (hiPSC)-derived neuronal cultures offer one potential platform to model and manipulate the network interactions of human neurons *in vitro*. In the 15 years since the original description of neural cell generation from patient-derived hiPSCs, numerous subsets of neurons and glial cells have been described and applied to the study of neurologic diseases ranging from neural developmental disorders to neurodegenerative disorders (Habela et al., 2016) (Shi et al., 2017). The advantages of these systems include an intact human genetic background with the ability to examine spontaneously as well as induced genetic variation, high-throughput platforms allowing for the study and manipulation of these processes, and the ability to manipulate cell types and cell numbers within a network (Nam et al., 2020).

The use of hiPSCs in both two-dimensional monolayer cultures and three-dimensional "organoid" cultures has revealed that cultured neurons generate spontaneous spikes and bursting activity, indicating functional and excitable neurons as well as synchronous network activity indicative of synaptically interconnected neurons in functional networks (Habibey et al., 2022) (Nam et al., 2020). More complex network behaviors such as cross-frequency coupling have not been previously described in two-dimensional (2D) cultures, but the presence of this activity *in vitro* in 2D cultures would offer an intermediate step between computational modeling and *in vivo* applications to generate and test hypotheses. We hypothesize that PAC is a fundamental and intrinsic property of human neuronal networks and therefore predict that it can be detected in human neurons *in vitro* independent of three-dimensional structure or external inputs.

2. Materials and methods

2.1. Cell culture

hiPSCs were maintained and passaged as previously described (Wen et al., 2014). Neural progenitor cells (NPCs) were generated using the human forebrain differentiation technique. For differentiation to human cortical neurons, NPCs were thawed onto poly-L-ornithine (PLO) and laminin-coated plates into Neuronal media consisting of Neurobasal Media (Thermofisher), Glutamax (Thermofisher), nonessential amino acids (Thermofisher), B27 supplement (Thermofisher), BDNF (10 ng/mL), GDNF (10 ng/mL) supplemented with 125 nM of the notch inhibitor Compound E (1:2000 DMSO) and 20 μM of Rho-associated coiled-coil forming protein serine/threonine kinase inhibitor (ROCK-I, compound Y-27632) (1:500 DMSO). After 48 hours, ROCK-I was removed, and Neuronal media supplemented with Compound E (125 nM) was completely exchanged every 48–72 hours until day in culture (DIC) 37 with every other media change containing 1 ug/mL laminin (Thermofisher). These cultures generate >99 % MAP2AB+ neurons (Wen et al., 2014).

For astrocyte differentiation, NPCs were thawed onto PLO and laminin-coated plates and cultured in astrocyte media supplemented with 1 % knockout serum replacement (KSR)(Thermofisher). Astrocyte progenitor cells (APCs) were passaged every 4–7 days with media changes every 48–72 hours. With the first passage, APCs were plated onto 1 % Matrigel (Corning) coated plates and maintained on Matrigel throughout subsequent passages. In preparation for co-cultures, APCs aged to DIC 77–86 were thawed onto PLO and laminin-coated plates in astrocyte media 1 % KSR until DIC 90 and the proportion of GFAP+ astrocytes was quantified by immunohistochemistry of sister cultures (90.8 ± SEM 0.6 %, n = 6 cultures).

2.2. Combined astrocyte and neuron co-culture

Neurons were aged to DIC 37 and synchronized with DIC 90–95 APCs. Cells were washed with sterile phosphate-buffered saline and lifted using 0.05 % Trypsin (Thermofisher) incubation at 37°C for 3 minutes. Neurons were resuspended for a final concentration of 50,000 cells per 5 μL in Neuronal media supplemented with 1 % anti-anti (GIBCO), 5 % KSR, 1:2000 compound E (MEA (Multielectrode Array) media) and 1:500 ROCK-I. Astrocytes were diluted to 25,000 cells per 5 μL in the same media as neurons. Neurons and astrocytes were combined 1:1 by volume for an astrocyte to neuron ratio of 1:2, approximating estimates for neuron and astrocyte composition of the human cortical grey matter (Herculano-Houzel, 2014). For multi-electrode array (MEA) recordings, 5 μL of the neuron and astrocyte suspension was placed as a droplet onto the center of a PLO and laminin coated 16 electrode array well of a 24 well MEA plate and incubated at 37°C, 5 % CO_2 for 20–30 minutes at before 500 μL of MEA media + ROCK- I was pipetted down the side of the well in two parts. ROCK-I was removed from the media after 48 hours and cocultures underwent partial media exchanges with MEA KSR twice a week until neuronal DIC 80 and subsequently once a week, with 1 ug/mL laminin added every other media change.

2.3. MEA recordings

Plates were equilibrated in the Axion Edge at 37°C, 5 % CO_2 for a minimum of 3 minutes prior to recording. Five-minute recordings were obtained at weekly or bi-weekly intervals beginning on DIC 42 until DIC 241. For bicuculline application experiments, recordings consisted of 3-minute baseline recordings. Recordings continued while the door to the machine was opened and 20 μL warmed media containing dimethyl sulfoxide (DMSO) was added to the culture well containing 1 mL culture media for a final DMSO concentration of 1:2000. Recording continued for 5–6 minutes prior to opening door to the machine and pipetting 20 μL media containing concentration 20 mM bicuculline stock sufficient for a 1:2000 dilution of the total well volume and a final calculated concentration of 10 μM bicuculline. Raw voltage and time data was exported to MATLAB format for CFC detection analysis. Discrete, non-continuous data based on spike count over time was analyzed by Axion software (AxisNavigator and Axion Neural Metric Tool) to generate average weighted mean firing rate, burst percentage and synchrony index per culture well.

2.4. Spike detection and sorting

To investigate the association between PAC and single cell spiking, we used an offline and unsupervised algorithm for spike detection and sorting using wavelets and super-paramagnetic clustering (Chaure et al., 2018). Recording from each individual electrode fed to two parallel pipelines, one for spike detection and sorting and the other for PAC analysis.

2.5. Instantaneous phase, frequency, and amplitude analysis

Raw voltage data from MEA recordings were analyzed using band-pass filtering in conjunction with the Discrete Hilbert Transform (DHT) to extract phase data from low frequency and amplitude from high frequency activity (Tort et al., 2010). The raw signals were filtered in the high-frequency (20–200 Hz) and low-frequency (1–10 Hz) frequency

bands using a zero-phase bandpass filter. Subsequently, the DHT was applied, which yielded an analytical function. The phase and absolute value of the analytic function from the filtered recording was used to calculate the instantaneous phase, frequency and amplitude.

2.6. Low-frequency phase modulated high-frequency amplitude

Phase amplitude coupling measures the degree to which the high-frequency power is modulated by the phase of the low-frequency oscillations. To quantify PAC, modulation index (MI) estimation was used (Tort et al., 2010, 2009, 2008). In summary, for the estimation of MI, the signal is filtered into two components - a lower frequency band to extract

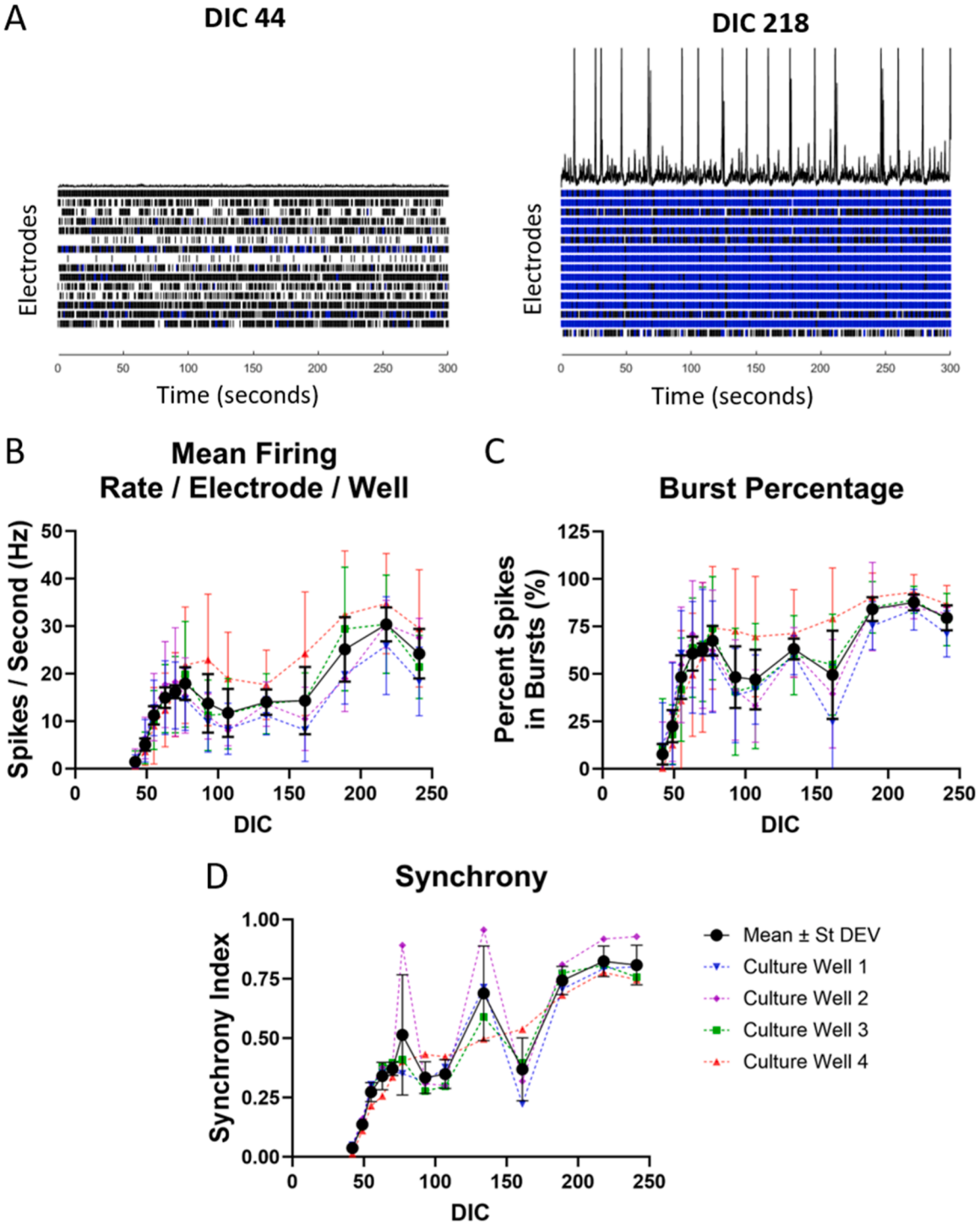

Fig. 1. Time course for the development of cultured human neurons and astrocytes. A. Raster plots representing spikes (black lines) and burst (blue lines) for each of 16 electrodes (rows) of a representative well at day in culture (DIC) 44 and 218. Spikes per time per second across all electrodes are illustrated at the top of each trace. B. Mean firing rate (MFR) calculated for each electrode and averaged for each well (colored traces, Mean ± SD). C. Average percent of spikes occurring in bursts per electrode per well for the same wells. D. The spike synchrony index for the same wells. Graphs represent data collected from four culture wells, each with 16 electrodes. Each data point is the mean of 16 electrodes ± standard error of the mean. Mean ± SD for all wells, black closed circles.

the phase and a higher frequency band to extract the amplitude. The instantaneous phase of the lower frequency component and the instantaneous amplitude of the higher frequency component are computed, using the Hilbert transform. The relationship between the phase of the lower frequency oscillation and the amplitude of the higher frequency oscillation is assessed. This is done by creating a phase-amplitude histogram, where the amplitude values are binned according to the phase at which they occur. The MI is calculated from this histogram. It quantifies the degree of coupling and is normalized to vary between 0 (no coupling) and 1 (maximum coupling). This is achieved by measuring the divergence of the observed amplitude-phase distribution from a uniform distribution, using statistical measures like the Kullback-Leibler divergence. A higher modulation index indicates a stronger coupling between the phase and amplitude signals, suggesting that the phase of the low-frequency signal has a greater impact on the amplitude of the high-frequency signal (Salimpour et al., 2022; Samiee and Baillet, 2017).

To track the changes in PAC over time, we used the mean modulation index (MMI). MMI is the average MI obtained in a sliding time window. It summarizes the MI results from a matrix to a vector in a specific time window. By moving the time window across the entire signal in small steps, we were able to capture and visualize the dynamic pattern of PAC changes over time. We used a sliding time window of 20 seconds with an advancing time step of 2 seconds to capture the dynamics of PAC. At each step, we used the MI method to measure PAC. We used MMI to generate a vector for each time point, which corresponded to the end of the sliding time window. By aligning the vectors associated with the end point of the sliding window, we created a dynamic pattern of PAC changes over time.

2.7. Statistical analysis

The MATLAB Statistical package was used. To assess the statistical significance of PAC changes, each experimental testing section, including a period during the retrieval phase, was analyzed using surrogate control analysis (Tort et al., 2010). We performed a statistical control analysis on each session by creating shuffled versions of the complex time series consisting of low-frequency phase and high-frequency amplitude. This generated surrogate MI values, from which the MI chance distribution could be inferred (Tort et al., 2010). One-sample and paired-sample t-test tests were used for mean MI changes, and a $P < 0.05$ was considered statistically significant (Dvorak and Fenton, 30 2014).

3. Results

3.1. Phase amplitude coupling in vitro

Human iPSC-derived human cortical neurons (hiPSC-CNs) in co-culture with hiPSC-derived human cortical astrocytes were grown in multi-well MEA plates. To monitor maturation, MEA plates were recorded every 1–2 weeks and multiunit spike data over time was extracted as demonstrated in example raster plots in Fig. 1A. Changes in activity were apparent over time. There was an initial rapid rise in the mean firing rate followed by a transient decrease and plateau around day in culture (DIC) 100 prior to increasing again to maximal firing between 20 and 40 Hz (Fig. 1B). The percentage of spikes occurring in bursts or burst percentage demonstrated an initial rapid rate of rise and then a plateau followed by more gradual increase and stabilization between 80 % and 90 % (Fig. 1C). The amount of synchronization across electrodes demonstrated a more gradual and variable rise (Fig. 1D) and like the burst percentage and mean firing rate, there was an eventual leveling off at maximal synchronization between DIC 193 and 241.

Continuous voltage data from recordings on DIC 218, when there appeared to be stable indicators of maximal maturation, showed that CFC exists in the form of PAC in two-dimensional cultures (Fig. 2). The raw voltage recording from a single representative electrode (Fig. 2A, gray trace) was subject to zero phase band pass filters in the low-frequency range of 1–10 Hz (Fig. 2A and B, red trace) and high-frequency range of 20–200 Hz (Figs. 2A and B, teal trace). Visual inspection of these traces suggests that the peak amplitude of the high frequency component is related to the phase of the low frequency oscillation (Fig. 2C). To determine if there is a coupling between low frequency phase and the amplitude of high frequency activity, the Hilbert transformation (Tort et al., 2010) was used. The phase values of low frequency activity (Fig. 2C, red trace) and the power of high frequency components (Fig. 2C, teal trace) were computed from the corresponding raw voltage over time in Fig. 2B. The time – frequency representation was used to set the range for exploring PAC (Cotic et al., 2011). Fig. 2D demonstrates the frequency component of the time segment from Fig. 2B and demonstrates a wide range of frequency components in the raw data.

To quantify PAC, the modulation index (MI)-based measurement was used (Tort et al., 2010). The results reveal a prominent level of PAC between the phase of low frequency activity (1 – 10 Hz) and the amplitude of high frequency activity (20–200 Hz) (Fig. 2E). In this example, the coupling is most pronounced in the low frequency range 1–2 Hz (highest intensity on heat map) (Fig. 2E). To verify the validity of PAC detection, a surrogate control analysis was used. This was accomplished by generating a new series of data that comes from maintaining the phase of the low frequency and shuffling the amplitude of the high frequency and estimating the modulation index based on these regenerated time series. This was replicated 100 times resulting in a significantly lower mean modulation index in the surrogate than is present in the original (one-sample t-test $P < 0.0001$) (Fig. 2F). This excludes a random origin of the observed PAC detection in our cultures (Tort et al., 2010).

3.2. Cross-frequency coupling across the network

To further validate the observed phenomenon of PAC in monolayer culture *in vitro*, additional electrodes from the same culture well and same timepoint shown in Fig. 2 were analyzed. Three additional representative electrodes are shown (Fig. 3A, top and bottom left) and the MI levels from all 16 electrodes were calculated (Fig. 3F, well 1 DIC 218). This demonstrates that CFC in the form of PAC is not limited to a single electrode and is detectable at all electrodes in the well at the DIC 218 timepoint. Additionally, similarities in PAC at different electrodes suggests that the phenomenon is a network phenomenon and not dependent on the cells located at that electrode. However, when data obtained at an earlier timepoint (DIC 44) from the same well illustrated in Figs. 2 and 3A (well 1) is analyzed a there is not CFC in the form of PAC (Fig. 3B). This is confirmed by the fact that there is no difference between the surrogate and original measures of PAC at DIC 44 (Fig. 3D) as was the case for the same well at DIC 218 (Fig. 2F) and an additional representative example (Fig. 3C and E). Further, there is a significant difference between the average PAC measures across 16 electrodes of well 1 between DIC 44 and DIC 218, but no difference between two different wells (well 1 and well 2) at the same DIC 218 timepoint (Fig. 3 F). This similar level of coupling in two independent wells at the same point in time suggests the presence of PAC is not unique to one particular culture and similar levels may be representative of similar stages of development.

3.3. Detection of dynamic changes using CFC

CFC detection and analysis can be considered an effective tool to assess the dynamic changes of cultured neurons at a network level. To evaluate whether dynamic changes can be captured *in vitro* using PAC, we analyzed baseline activity as well as the changes occurring with the addition of the Gama-aminobutyric acid (GABA) receptor antagonist, bicuculline or vehicle control. Application of 10 μM bicuculline during

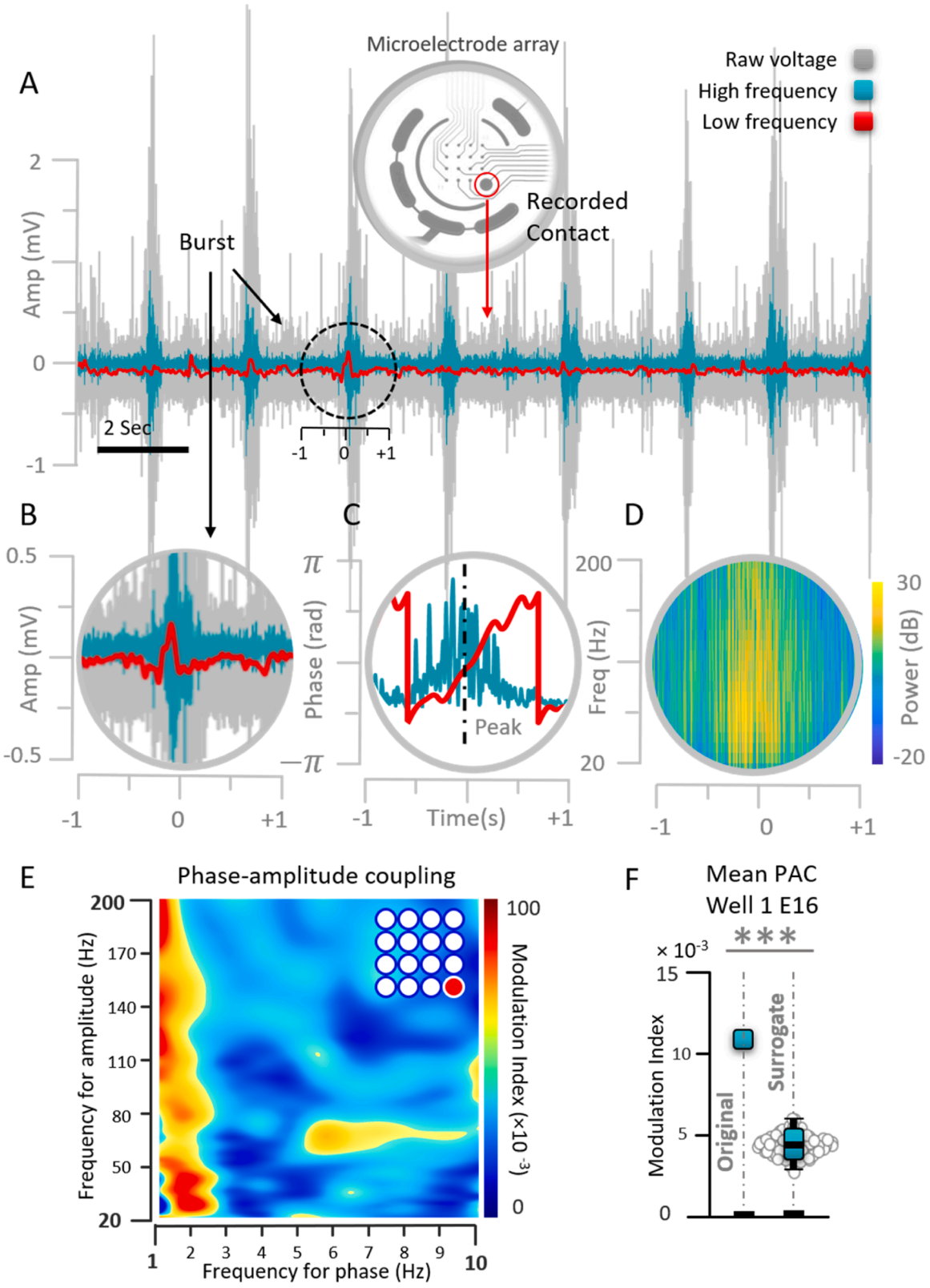

Fig. 2. Frequency analysis in multi-electrode array recordings. A. Sample recording from a single electrode of a microelectrode array. Raw local field potential is grey. Zero phase bandpass filtering of data in low frequency range (1–10 Hz) in red and high frequency range (20–200 Hz) in teal. B. Amplification of the dashed circle in A. Visual inspection of these traces suggests a typical signature of cross-frequency coupling (CFC) in the format of the phase-amplitude coupling (PAC). C. Phase decomposition of the low frequency (red) and power decomposition of the high frequency range (teal) corresponding to the voltage traces in B shows the association between the peak of the phase in low frequency (dashed line) and the power of high frequency components. D. The time – frequency representation shows a wide range of frequency components in the raw voltage data associated with the sample burst demonstrated in panel B. E. The modulation index measure is used to quantify and visualize PAC in the same electrode. F. Significant differences between estimated mean PAC (MI = 0.0127) and a set of 100 randomly created shuffled versions of the low-frequency phase and high-frequency amplitude (0.0043 ± 0.0082, $P < 0.0001$).

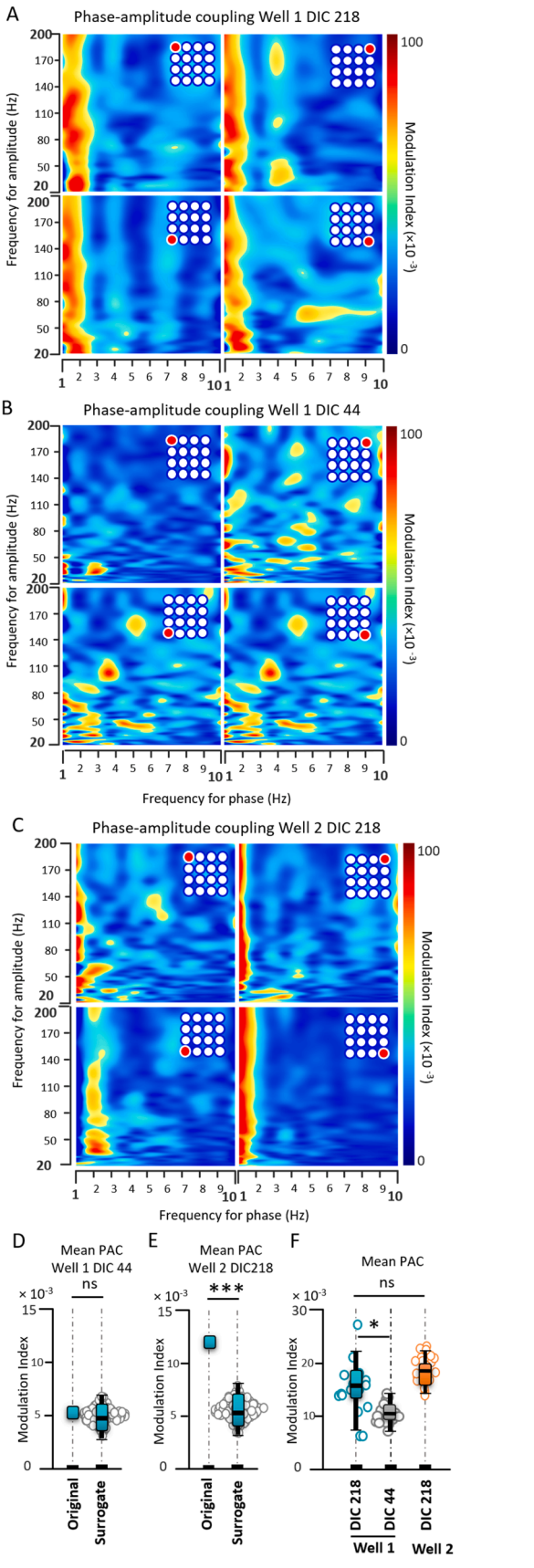

(caption on next column)

Fig. 3. Cross frequency coupling (CFC) at the Network Level. CFC in the form of phase-amplitude coupling (PAC) detected across an entire well. A. Three additional electrodes from the same culture well (well 1) in Fig. 2 at day in culture (DIC) 218 are shown. B. PAC analysis of 4 electrodes from well 1 at DIC 44. C. The results of PAC analysis from well 2 at DIC 218. D. The mean PAC measure for a representative electrode of Fig. 3B (well 1, DIC44) is compared to the mean of the surrogate data and there is no significant difference between surrogate (0.0049 ± 0.0072) and original measures (0.0053) ($P = 0.1514$). E. The mean PAC measure of a representative electrode from the well in panel C (well 2, DIC 218) compared to the mean of the surrogate data demonstrating a significant difference between the surrogate (0.0057±0.0092) and original measures (0.0125) ($P < 0.0001$). F. The mean PAC measures across the entire well (16 electrodes) compared between a single well at two timepoints (well 1) and two wells at the same timepoint (well 1 vs well 2 at DIC 218). The mean of the PAC measures from well 1 at DIC 218 (0.0136 ± 0.0049) (teal – left) is significantly different from the PAC level measured from the same well at DIC 44 (0.0079± 0.0015) ($P = 0.034$) (grey- middle) and there is no significant difference between PAC levels in well 1 and well 2 (orange – right) (0.0111 ± 0.0025) ($P = 0.110$) when both cultures are aged to DIC 218.

continuous recording results in changes in the raw multiunit neuronal firing patterns (Fig. 4A blue trace). A different pattern was present when media containing vehicle was applied (Fig. 4A red trace). When the period prior to drug (Baseline 2) or vehicle application (Baseline 1) (left) is compared to the period after drug application (right), a change in the PAC is evident with a shift in the frequency of the low frequency driving the high frequency in response to bicuculline addition. (Fig. 4B right panels) that is not as clearly evident with the addition of vehicle to the cultures (Fig. 4B, left panels). In order to quantify this change, the mean PAC measures across the entire well (16 electrodes) for the three representative wells demonstrated in Fig. 4B were averaged to generated a single MI value for each well at each low-frequency oscillation (1–5 Hz) (Fig. 4C). At baseline and in response to vehicle application the peak modulation index (MI) values are at 1 Hz and there is not a significant change in the average MI values between baseline and vehicle addition. Bicuculline addition results in a nonsignificant decrease in the MI values at 1 Hz ($P = 0.0598$) and a significant increase at 2 Hz ($P = 0.0277$).

Dynamic changes in PAC over time can be demonstrated by sliding windows based dynamic PAC analysis (Salimpour et al., 2022; Samiee and Baillet, 2017) in which the high frequency amplitude across all low frequency amplitudes is analyzed over time. We applied this analysis to the raw multi-unit potential data in Fig. 5A. The analysis in Fig. 5B demonstrates that, although there are fluctuations in the coupling with increased MI values at some, but not all high frequencies prior to bicuculine administration, at the time of bicuculline administration there is a change in the PAC characterized by a transient increase in coupling at all frequencies resulting in an overall increased mean modulation index followed by a decrease in coupling. This suggests dynamic fluctuations in synchronization.

To study the relationship between dynamic network activity and single cell activity, offline spike sorting of the raw voltage data was performed (Chaure et al., 2018). At the single-cell level, bicuculline application results in an increase in the firing rate and more tonic activity in some neurons (Fig. 5C, top), while other neurons have significantly reduced firing or stop firing all together (Fig. 5C, bottom). These changes in firing rate appear to occur at the same time or just prior to the increase in MI across all frequencies in the dynamic PAC analysis presented in Fig. 5B. However, the changes in individual neuronal firing patterns outlast the transient increase in PAC.

4. Discussion

In this study, we investigated the formation of phase-amplitude coupling (PAC) in hiPSC-derived human cortical neurons in 2D cultures *in vitro*. The results demonstrate that, like the human brain *in vivo*, cross frequency coupling (CFC) is present in the form of PAC *in vitro*. This

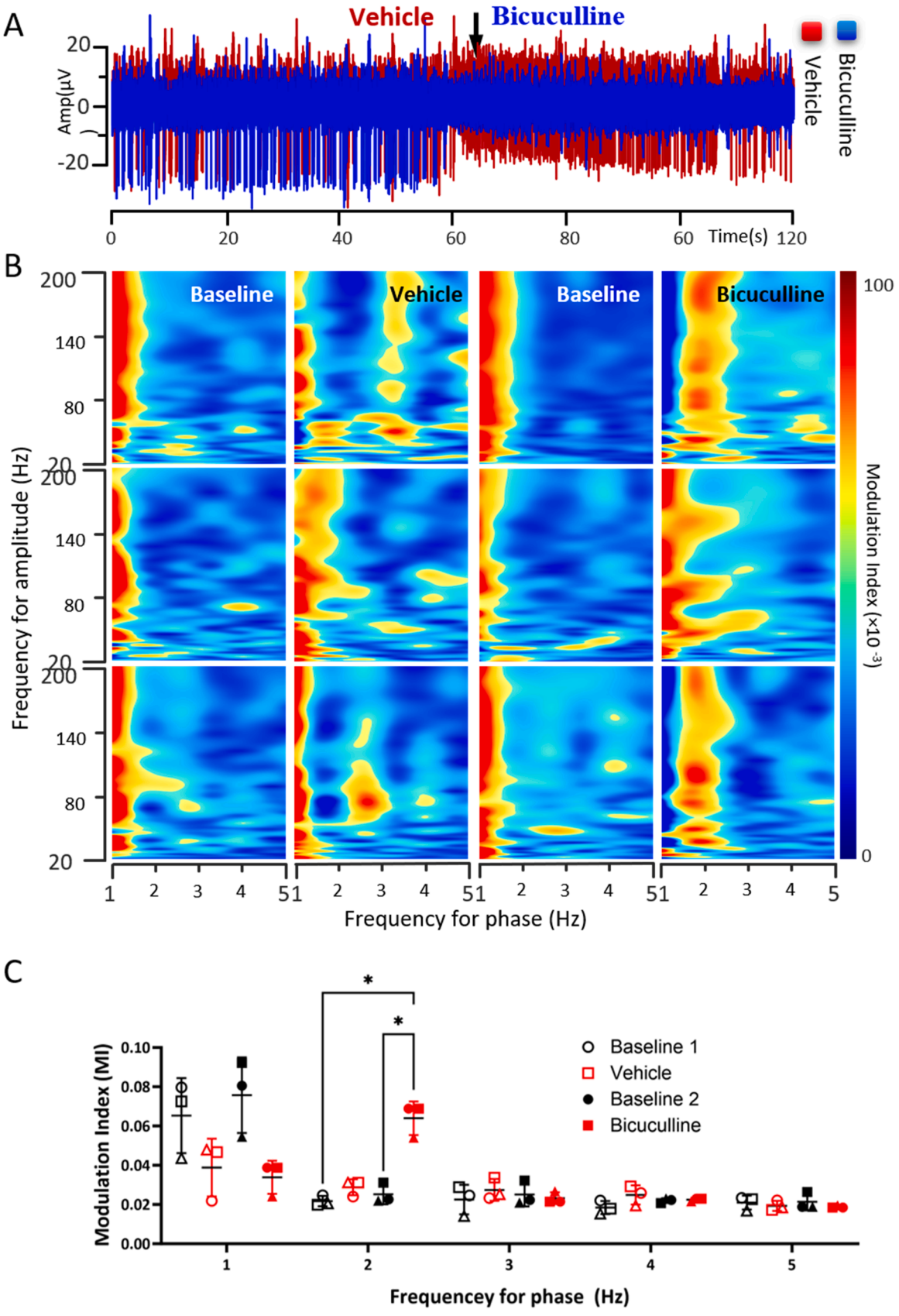

(caption on next page)

Fig. 4. Cross frequency coupling (CFC) dynamics. A. Application of bicuculline (10 μM) (blue) or vehicle (red trace) as indicated by black arrow, results in a change in the raw multi-unit neuronal firing patterns. The waveforms are aligned based on the time of bicuculline, and vehicle administration. B. Modulation index (MI)-based quantification of phase-amplitude coupling was performed using data from pre-time and post-time periods of bicuculline, and vehicle administration. The sample phase amplitude coupling (PAC) measures from representative electrodes were recorded from three different wells (top panel, middle panel and bottom panel). C. The mean PAC measures across the entire well (16 electrodes) for three representative wells averaged by well and summarized based on the frequency of low-frequency oscillations (1–5 Hz). Open symbols represent Baseline 1 and Vehicle application. Closed symbols are bicuculline and baseline 2. Shapes are individual wells across all conditions. Line is the mean ± SD. The mean PAC peak at baseline is at 1 Hz (0.065± 0.019) and is not significantly different from the PAC level measured in the same frequency after adding media containing vehicle ($P = 0.573$).Application of bicuculline results in a nonsignificant reduction in mean PAC at 1 Hz compared to Baseline 2 ($P = 0.0598$) shifts the peak PAC coupling to 2 Hz where the MI level is significantly greater after treatment with bicuculline (0.064 ± 0.009) in comparison to the baseline 2 (0.025± 0.005) ($P < 0.027$) (Two- way ANOVA, Tukey's multiple comparison's test. * $P < 0.05$, unless otherwise specified all comparisons between conditions at each frequency $P > 0.05$).

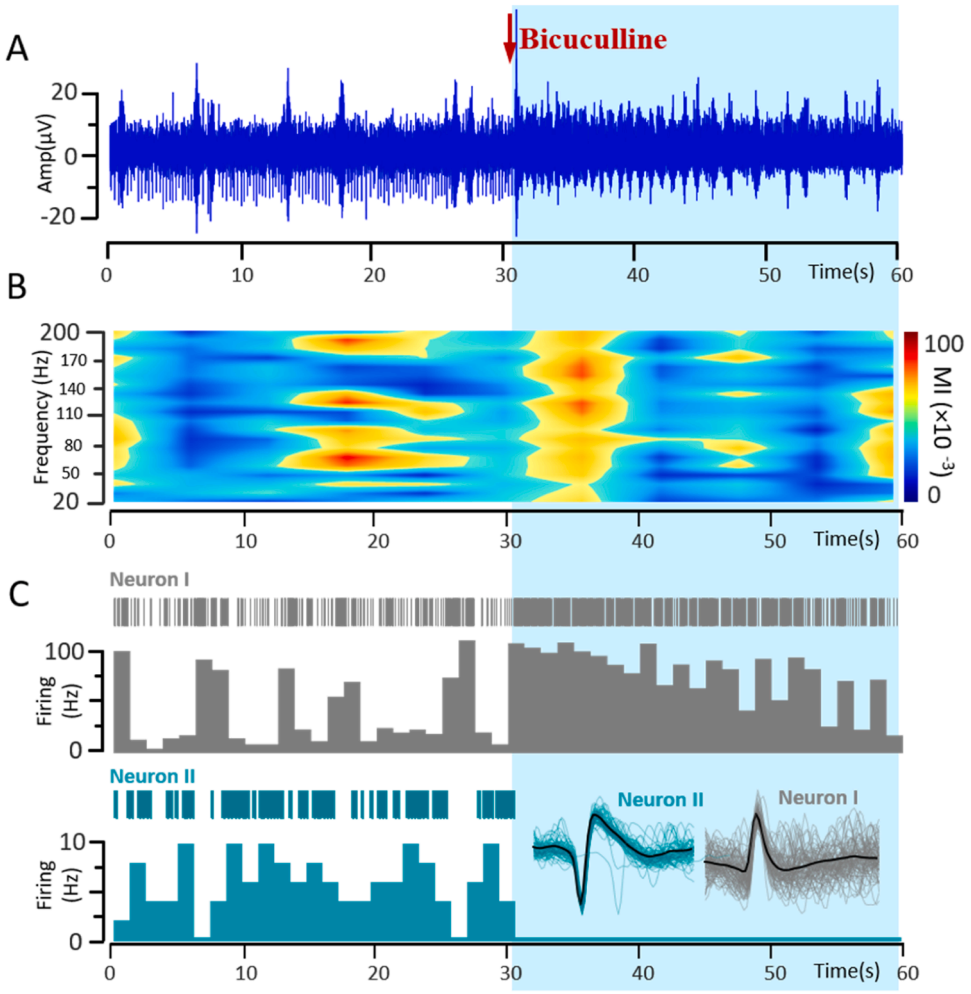

Fig. 5. Cross frequency coupling (CFC) - reflection at the single cell level. A. Application of bicuculline (10 μM), (red arrow and blue shading), results in changes in the raw multi-unit neuronal firing patterns. B. Dynamic changes in phase amplitude coupling (PAC) over time demonstrated by sliding windows based dynamic PAC analysis in which the high frequency amplitude across all low frequency amplitudes is analyzed over time. C. Example neurons from spike sorting of the local field potential recording from a single electrode. For each neuron, a raster plot of spikes over time (top line) is presented above the firing frequency over time at timepoints prior to and after bicuculline administration. Individual spike waveforms of Neuron I (grey) and Neuron II (teal) and the average waveform (black) are shown at bottom right.

coupling is a property of the network of individual cultures with similar PAC across different electrodes in the same well. PAC may be a developmental phenomenon as it is absent at time points when networks are likely to be immature and present to similar degrees in different

cultures of the same age. Additionally, the presence of PAC is dynamic and can be modulated by chemical manipulation of neuronal synaptic interactions. Finally, simultaneous analysis of single cell properties and PAC suggests that changes in PAC are not driven by the single cell properties of one neuron but rather the interactions between neurons.

Neuronal oscillations of different frequencies in the cortical and subcortical structures demonstrate complicated coupling properties reflecting more complex features of neural oscillations present in the brain's normal activities, mostly in CFC in the form of PAC (Canolty and Knight, 2010). CFC formation in hiPSC based neuronal cultures supports the theory that complicated neuronal oscillations are inherent properties of neuronal networks. The presence of PAC in human neuronal culture *in vitro* suggests that the intrinsic interactions between individual cells are sufficient to produce a specific level of local PAC without external influences. Phase amplitude coupling between delta oscillations

has been described in 3-dimensional brain organoid cultures (Trujillo et al., 3 2019) and neuronal spiking in brain organoids has also been shown to be phase locked to theta oscillations (Sharf et al., 2022). However, the phenomenon of PAC has not previously been described in 2D human cultures. The existence of PAC in 2D cultures suggests that PAC is a fundamental property of neural networks and is independent of 3D structure. Importantly, the presence of this phenomenon *in vitro* offers the possibility of a model system that can be used to further define the underlying determinants of PAC and its dynamics. Compared to 3D cultures, 2D cultures may provide specific advantages for future exploration including the ability to titrate the ratio of inhibitory to excitatory cells, genetically manipulate different cell types within the same cell culture system or examine the effects of non-neuronal cells such as astrocytes on PAC.

Although the neural mechanism underlying PAC in the brain is not fully understood, current evidence shows the contribution of both pyramidal cells and interneurons, which fire simultaneously at specific phases of low-frequency oscillation (Hyafil et al., 2015). The culture technique used here generates glutamatergic forebrain specific neurons with 5–10 % GABAergic neurons (Wen et al., 2014). The change in multiunit and single unit firing rates in response to application of the GABA receptor antagonist, bicuculline demonstrates that there are functional GABAergic synapses in these networks. Importantly, the shift in the frequency for phase of the PAC in response to bicuculline confirms that synaptic GABAergic activity modulates the coupling. However, the fact that the change does not correlate with a simple increase or decrease in firing rate of individual neurons indicates that this phenomenon reflects network processing. This hypothesis is supported by the presence of PAC in mature, but not immature cultures, although the exact developmental time course and the type of processing that this reflects will need to be evaluated further in future studies. *In vitro* 2D culture systems are potentially ideal model systems to study the contributions of both excitatory and inhibitory neurons to this process. Our evidence demonstrates the potential of CFC analysis to capture the dynamics of neuronal interactions at the network level and potentially explore the effects of different neuromodulation modalities such as chemical, electrical, and even ultrasound in the future.

HiPSC-derived neurons offer the potential for the development of cell therapies, drug discovery, and disease modeling. However, the extent to which *in vitro* populations of neurons can recapitulate the complex network interactions that are present in the brain *in vivo* is not fully understood. Disruption of these interactions, that is not necessarily evident in single-cell properties, may be the underlying pathology in numerous disease models such as epilepsy and PD. Application of neuronal network analysis in hiPSC-derived neuronal cultures provides a unique opportunity for investigating the neuronal mechanisms underlying complicated behavior of neuronal populations. It adds another dimension to the analysis of hiPSC-derived neurons and provides the potential to enhance our understanding of complex oscillatory behavior in neuronal information processing.

Author contributions

YS: performed analysis, wrote first draft, conceptualized experiments and contributed to the final draft of the manuscript, WA: conceptualized experiments and contributed to the final draft of the manuscript. RD contributed to analysis and writing. SL contributed to experiments. HS: contributed materials and to experimental protocols and analysis and writing. G-LM: contributed materials and to experimental protocols and analysis and writing. NM: conceptualized experiments and contributed to the final draft of the manuscript, provided materials and supervised the project. CWH performed experiments, analysis and wrote first draft of manuscript, conceptualized experiments and wrote the final draft of the manuscript, provided materials and supervised the project.

CRediT authorship contribution statement

Christa Whelan Habela: Conceptualization, Data curation, Formal analysis, Resources, Supervision, Writing – original draft, Writing – review & editing. **Shiyu Liu:** Writing – review & editing, Methodology, Data curation. **Guo-Li Ming:** Investigation, Resources, Writing – review & editing. **Hongjun Song:** Methodology, Resources, Writing – review & editing. **Nicholas J Maragakis:** Funding acquisition, Investigation, Resources, Supervision, Writing – review & editing. **Yousef Salimpour:** Writing – review & editing, Writing – original draft, Methodology, Formal analysis, Data curation, Conceptualization. **William S Anderson:** Writing – review & editing, Supervision, Resources, Conceptualization.

Declaration of Competing Interest

The authors declare no competing financial interests

Data availability

Data will be made available on request.

Acknowledgements

CNCDPK12, K08NS102526, Doris Duke Foundation Clinical Scientist Award to CWH; NIH 5R01NS117604 and Department of Defense ALSRP W81XWH1810175 to N.J.M.; NIH R35NS116843 to H.S. and NIH R35NS097370 to G-l.M.

References

Canolty, R.T., Knight, R.T., 2010. The functional role of cross-frequency coupling. Trends Cogn. Sci. 14 (11), 506–515. https://doi.org/10.1016/j.tics.2010.09.001.

Cash, S.S., Hochberg, L.R., Apr 8 2015. The emergence of single neurons in clinical neurology. Neuron 86 (1), 79–91. https://doi.org/10.1016/j.neuron.2015.03.058.

Chaure, F.J., Rey, H.G., Quian Quiroga, R., 2018. A novel and fully automatic spike-sorting implementation with variable number of features. J. Neurophysiol. 120 (4), 1859–1871. https://doi.org/10.1152/jn.00339.2018.

Cotic, M., Chiu, A.W., Jahromi, S.S., Carlen, P.L., Bardakjian, B.L., Aug 2011. Common time-frequency analysis of local field potential and pyramidal cell activity in seizure-like events of the rat hippocampus. J. Neural Eng. 8 (4), 046024 https://doi.org/10.1088/1741-2560/8/4/046024.

Dvorak, D., Fenton, A.A., Mar 30 2014. Toward a proper estimation of phase-amplitude coupling in neural oscillations. J. Neurosci. Methods 225, 42–56. https://doi.org/10.1016/j.jneumeth.2014.01.002.

Habela, C.W., Song, H., Ming, G.L., Jun 2016. Modeling synaptogenesis in schizophrenia and autism using human iPSC derived neurons. Mol. Cell Neurosci. 73, 52–62. https://doi.org/10.1016/j.mcn.2015.12.002.

Habibey, R., Striebel, J., Schmieder, F., Czarske, J., Busskamp, V., 2022. Long-term morphological and functional dynamics of human stem cell-derived neuronal networks on high-density micro-electrode arrays. Front Neurosci. 16, 951964-951964. doi:10.3389/fnins.2022.951964.

de Hemptinne, C., Ryapolova-Webb, E.S., Air, E.L., et al., 2013. Exaggerated phase-amplitude coupling in the primary motor cortex in Parkinson disease. Proc. Natl. Acad. Sci. 110 (12), 4780–4785. https://doi.org/10.1073/pnas.1214546110.

Herculano-Houzel, S., Sep 2014. The glia/neuron ratio: how it varies uniformly across brain structures and species and what that means for brain physiology and evolution. Glia 62 (9), 1377–1391. https://doi.org/10.1002/glia.22683.

Hyafil, A., Giraud, A.-L., Fontolan, L., Gutkin, B., 2015. Neural cross-frequency coupling: connecting architectures, mechanisms, and functions. /11 2015 Trends Neurosci. 38 (11), 725–740. https://doi.org/10.1016/j.tins.2015.09.001.

Nam, K.H., Yi, S.A., Jang, H.J., Han, J.-W., Lee, J., 2020. In vitro modeling for inherited neurological diseases using induced pluripotent stem cells: from 2D to organoid. /08/05 2020 Arch. Pharmacal Res. 43 (9), 877–889. https://doi.org/10.1007/s12272-020-01260-z.

Salimpour, Y., Anderson, W.S., 2019. Cross-frequency coupling based neuromodulation for treating neurological disorders. Front Neurosci. 13, 125-125. doi:10.3389/fnins.2019.00125.

Salimpour, Y., Mills, K.A., Hwang, B.Y., Anderson, W.S., 2022. Phase- targeted stimulation modulates phase-amplitude coupling in the motor cortex of the human brain. /01 2022 Brain Stimul. 15 (1), 152–163. https://doi.org/10.1016/j.brs.2021.11.019.

Samiee, S., Baillet, S., 2017. Time-resolved phase-amplitude coupling in neural oscillations. NeuroImage 159, 270–279.

Sharf, T., van der Molen, T., Glasauer, S.M., et al., 2022. Functional neuronal circuitry and oscillatory dynamics in human brain organoids. Nat. Commun. 13 (1), 4403.

Shi, Y., Inoue, H., Wu, J.C., Yamanaka, S., 2017. Induced pluripotent stem cell technology: a decade of progress. Nat. Rev. Drug Discov. 16 (2), 115–130. https://doi.org/10.1038/nrd.2016.245.

Tort, A.B.L., Komorowski, R., Eichenbaum, H., Kopell, N., 2010. Measuring phase-amplitude coupling between neuronal oscillations of different frequencies. J. Neurophysiol. 104 (2), 1195–1210. https://doi.org/10.1152/jn.00106.2010.

Tort A.B., Komorowski R.W., Manns J.R., Kopell N.J., Eichenbaum H. Theta-Gamma Coupling Increases During the Learning of Item-context Associations. Proc Natl Acad Sci U S A. Dec 8 2009;106(49):20942-7. doi:10.1073/pnas.0911331106.

Tort, A.B., Kramer, M.A., Thorn, C., et al., 2008. Dynamic cross-frequency couplings of local field potential oscillations in rat striatum and hippocampus during performance of a T-maze task. Dec 23 Proc. Natl. Acad. Sci. 105 (51), 20517–20522. https://doi.org/10.1073/pnas.0810524105.

Trujillo, C.A., Gao, R., Negraes, P.D., et al., Oct 3 2019. Complex oscillatory waves emerging from cortical organoids model early human brain network development. e7 Cell Stem Cell 25 (4), 558–569. https://doi.org/10.1016/j.stem.2019.08.002.

Wen, Z., Nguyen, H.N., Guo, Z., et al., 2014. Synaptic dysregulation in a human iPS cell model of mental disorders. Nature 515 (7527), 414–418.